

## Assessing methods for estimating roughness coefficient in a vegetated marsh area using Delft3D

Khalid Al-Asadi and Jennifer G. Duan

### ABSTRACT

A Delft3D-FLOW model was used to simulate tidal flow in Davis pond marsh in Louisiana, USA. The study area is a freshwater marsh consisting of one main channel and floodplain. Vegetation-induced flow resistance greatly influences tidal flow dynamics in the marsh. This study evaluated eight approaches to estimate vegetation roughness, including two constant Manning's  $n$  values, four empirical relations for calculating  $n$ , and two methods for calculating Chezy's  $C$  values originally embedded in the Delft3D model. Simulated results of water surface elevation (WSE) were compared with the corresponding field observation at eleven stream gauges in the study area. We concluded that the roughness coefficient for vegetated area varies with time as flow depth changes. Among the selected empirical relations for the vegetation roughness, the ones accounting for the effect of the vegetation frontal area and the degree of submergence have closely matched the measurements.

**Key words** | Delft3D model, hydrodynamic model, Manning's roughness, vegetation density, vegetation resistance

**Khalid Al-Asadi**  
**Jennifer G. Duan** (corresponding author)  
 Department of Civil Engineering and Engineering  
 Mechanics,  
 University of Arizona,  
 Tucson,  
 Arizona,  
 USA  
 E-mail: [gduan@email.arizona.edu](mailto:gduan@email.arizona.edu)

**Khalid Al-Asadi**  
 Department of Civil Engineering,  
 University of Basrah,  
 Basrah, Iraq

### NOTATION

The following symbols are used in this paper:

$a$	the frontal area of vegetation stem per unit volume ( $\text{m}^{-1}$ );	$n_1, n_2$	the maximum Manning's coefficient for vegetated channels ( $\text{s}/\text{m}^{1/3}$ );
$B$	surface width (m);	$N$	total number of observed WSE;
$B^V, B^X$	volumetric and cross-section blockage factors, respectively (–);	$O_i$	$i$ th value of observed WSE;
$C$	Chezy's coefficient ( $\text{m}^{1/2}/\text{s}$ );	$\bar{O}_i$	average value of the observed WSE;
$C_b$	Chezy's coefficient for non-vegetated channel ( $\text{m}^{1/2}/\text{s}$ );	$S_i$	$i$ th value of the simulated WSE;
$C_D$	drag coefficient (–);	$u_{v0}$	average velocity in the vegetation zone (m/s);
$C^*$	coefficient for the shear stress at the interface between vegetated and non-vegetated zones (–);	$V$	averaged velocity across the flow depth (m/s);
$g$	gravity acceleration ( $\text{m}/\text{s}^2$ );	$w$	vegetation frontal width (m);
$H$	flow depth (m);	$z_0$	length scale of bed roughness (m);
$h_v$	height of vegetation (m);	$\alpha$	coefficient (–);
$m$	vegetation density ( $\text{stem}/\text{m}^2$ );	$\beta$	vegetation resistance parameter ( $\text{s} \cdot \text{m}^{1/6}$ ) 0.4 (for sparse, low density vegetation $H > 0.3$ m); 1.6 (for moderately dense vegetation $H = 0.3$ m); 6.4 (for very dense vegetation $H < 0.3$ m); and turbulence length scale (m);
$n$	Manning's coefficient ( $\text{s}/\text{m}^{1/3}$ );	$\eta$	von Karman constant 0.41 (–);
$n_o, n_1$	the maximum Manning's coefficient for non-vegetated channels ( $\text{s}/\text{m}^{1/3}$ );	$\kappa$	parameter relating to vegetation resistance;
		$\lambda$	density of water ( $\text{kg}/\text{m}^3$ ).
		$\rho$	

doi: 10.2166/hydro.2017.064

## INTRODUCTION

Vegetation alters velocity profile and flow resistance in open channel flow through individual branch and blade on a single plant, or a community of plants as patch or canopy in a channel reach (Nepf 2012). Vegetation-induced flow resistance is dependent on vegetation coverage, namely the blockage factor (Green 2005), defined as the percentage of channel cross-sectional area, or surface area, or volume filled with vegetation. Figure 1 shows one vegetated cross-section in a channel. The height of vegetation is  $h_v$ , and its frontal width is  $w$ . Flow depth is  $H$ , and surface width is  $B$ . The percentage of vegetation occupied cross-section area is the cross sectional blockage factor. The product of vegetation density in stems per unit area and its frontal width is defined as  $\alpha$ . It is worth mentioning that Fisher (1992) first examined the differences of using surface area and volume to quantify the blockage factor, and recommended the percentage of surface area for the blockage factor because it is easier to measure. Recently, Green (2005), Nikora *et al.* (2008), and Luhar & Nepf (2013) used the percentage of cross-sectional area occupied by vegetation as the blockage factor. Since the cross-section based blockage factor better represents the intensity of turbulence wake in vegetation zones, it is more closely correlated with the resistance than the surface area based blockage factor.

Early researchers (e.g. Ree & Palmer 1949; Cowan 1956; Chow 1959; Petryk & Bosmajian 1975) formulated many empirical relations for Manning's roughness coefficient correlating with flow and vegetation properties. However, these relations are only applicable to limited vegetation types and

experimental flow conditions (e.g. flow depth) (Klopstra *et al.* 1997; Wu *et al.* 1999; Abood *et al.* 2006). SED2D model, a depth averaged two-dimensional hydrodynamic model, has included an empirical formula to calculate Manning's  $n$  for channels with vegetation. The  $n$  value in SED2D model is a function of the maximum  $n$  value for channel free of vegetation, vegetation height, flow depth, and the maximum  $n$  value of vegetated water (Letter *et al.* 2011). Through measuring turbulence around vegetation, researchers (e.g. Nepf *et al.* 1997; Nepf 1999) found bed shear stress affected near-bed turbulence production, while far away from the bed, the turbulence wake generated by stems becomes dominated (Nepf *et al.* 1997). The vortex from the stem wake extracts energy from the mean flow, and feeds it into turbulence kinetic energy (Nepf 1999). Consequently, turbulence intensity initially increases with stem density, and then reaches a peak at a given vegetation density, but eventually subsides as the density becomes very high (Nepf *et al.* 1997).

However, to date, there is no consensus on which method is the most feasible for calculating Manning's  $n$  in freshwater marshes. Vegetation-induced resistance is highly variable in the field due to complex vegetation types, density, and height. To quantify these varieties, we selected the Delft3D-Flow, a widely used open source three-dimensional hydrodynamic model, to study vegetation impact on tidal flow hydrodynamics.

## FLOW MODEL

The Delft3D-FLOW open source program (<http://oss.deltares.nl/web/delft3d/source-code>) is a three-dimensional

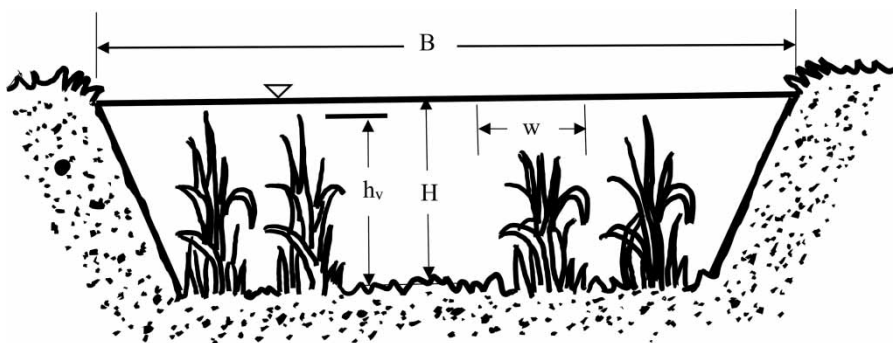


Figure 1 | Schematic of blockage factor in vegetated channel.

(3D) hydrodynamic and sediment transport model capable of simulating unsteady incompressible flow (Deltares 2011). The Reynolds Averaged Navier–Stokes equations, under shallow water (hydrostatic pressure) assumption, were solved using a finite difference scheme on a structured staggered curvilinear grid (Stelling & van Kester 1994). Delft3D-FLOW allows users to choose from two vertical grid systems:  $\sigma$ -grid and Z-grid, and four turbulence closure models: constant eddy viscosity coefficient, algebraic eddy viscosity model,  $k$ - $L$  model, and  $k$ - $\epsilon$  model.

Delft3D-FLOW has a function, Trachytopes, for users to define bed and flow resistance on each sub-grid (Deltares 2011). Three classes are available in the Trachytopes function: area, line, and point class. The area class has three types: the first is a constant coefficient for bed roughness, such as White Colebrook, Chezy, and Manning's coefficients, the second accounts for form resistance resulting from sand dunes, and the third is for calculating roughness coefficient in vegetated channels. In a simulation run, the roughness coefficient often remains a constant with time if choosing the first type of area class, while for the second type, it is determined by dune height, and the third by vegetation properties. The line class of Trachytopes function is used to approximate flow resistance for elements with hedge, bridge piers, and other structures. The point class is used to represent a set of point flow resistance elements, such as groups of individual trees or small plant.

Delft3D-Flow has incorporated vegetation effect through an adjusted bed roughness. For example, an implementation based on Klopstra *et al.* (1996) was added to the Klopstra *et al.* (1997) equation for calculating the  $C$  value of emergent vegetation (Deltares 2011) (Table 2). Additionally, an artificial term was added to account for extra momentum loss due to vegetation using Baptist's (2005) equation (Table 2). Furthermore, the momentum equations and the  $k$ - $\epsilon$  turbulent closure model in Delft3D-FLOW have been modified to include vegetation-induced momentum loss as well as influences of vegetation on turbulence generation and dissipation.

Temmerman *et al.* (2005) studied the vegetation impact on flow hydrodynamic and sedimentation processes in a tidal creek within the Paulina salt marsh in the Scheldt estuary, located at the southwest of Netherland, by modifying the momentum and  $k$ - $\epsilon$  equations in Delft3D-FLOW. Lately, Horstman *et al.* (2013) used Delft3D-FLOW for modeling

the tidal dynamics in the mangrove forest in Trang Province, Thailand. Both cases are in saltwater marshes where tidal flow is dominant, and vegetation types are distinct from ones in freshwater marshes. None of them have compared the model's performances with results using other methods not embedded in Delft3D to improve their modelling results.

The objective of this study is to evaluate the accuracy of different methods for calculating vegetation-induced roughness. The methods are not limited to the ones programmed in Delft3D, but all the methods available in literature. Therefore, the first and third types of area class in the Trachytopes function were adopted for incorporating other methods to calculate vegetation-induced roughness. Besides, we selected the orthogonal curvilinear coordinate system, and the vertical plane is  $\sigma$ -grid. The  $k$ - $\epsilon$  model was chosen to determine the coefficient of eddy viscosity. The sensitivity of modeling results to the selection of vertical grid and key parameters (e.g.  $a$  value) was analyzed.

## DESCRIPTION OF STUDY SITE

The study site is a vegetated freshwater marsh in Davis pond, located west of the Mississippi River and southwest of New Orleans, LA (Figure 2). Natural and man-made levees have reduced freshwater, sediment, and nutrient input from the Mississippi River to the surrounding estuarine marsh areas (McAlpin *et al.* 2008). This causes an intrusion of saltwater that threatens the existing freshwater habitat. To reduce the effects from saltwater intrusion, the Davis pond project was constructed to divert freshwater from the Mississippi River into the adjacent estuarine areas. When the project began to operate, unexpected high water levels were observed throughout the study area. To manage the water level, McAlpin *et al.* (2008) studied the causes by simulating the study site applying RMA2 model. McAlpin *et al.* (2008) validated the model by comparing the simulated water surface elevations (WSEs) with the observed, and proposed 12 alternatives to reduce water level.

The study site is surrounded by levees at the north, east, and west, and a gabion rock weir along the Lake Cataouatche shoreline on the south boundary. The inlet canal connects the pond with the Mississippi River, and provides freshwater to the pond. Water in the pond flows into Lake Cataouatche through the weir. The area is covered with a significant

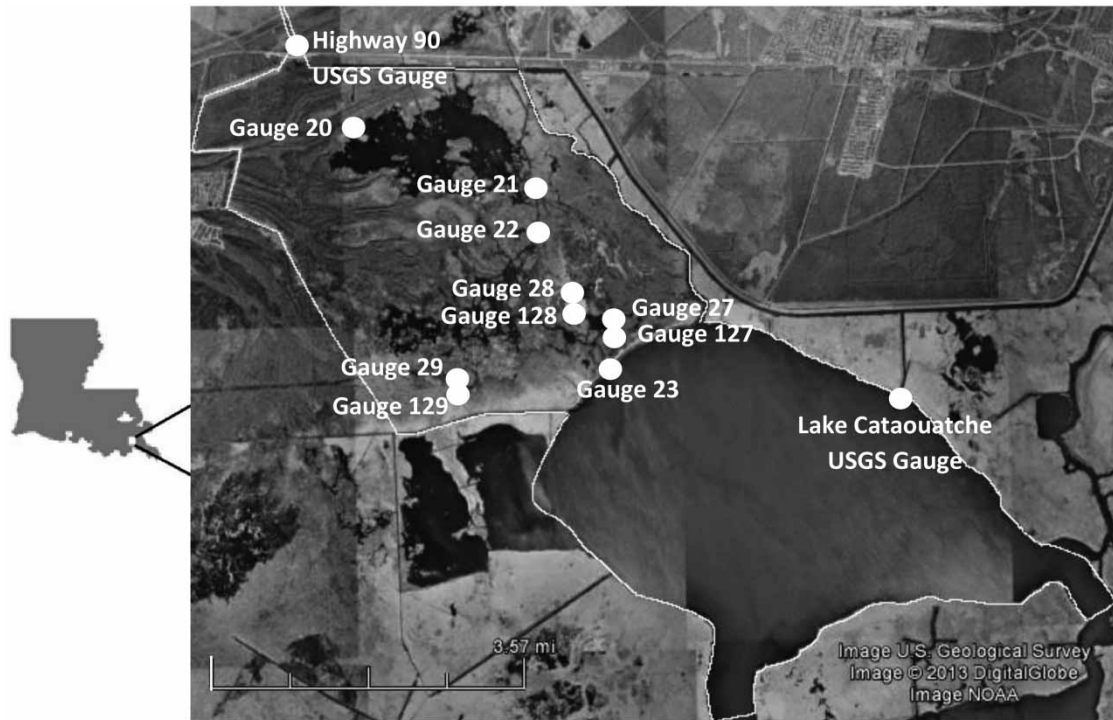


**Figure 2** | Location of study area, Highway 90, and Lake Cataouatche, and USGS gauges.

amount of freshwater marsh of typical vegetation, such as *Panicum hemitomon* (Sasser *et al.* 2008). A previous study (O'Neil 1949) found that *Panicum hemitomon* is typical in freshwater marshes in the Mississippi River delta. The mature *Panicum hemitomon* has a stem height about 0.762 m, and a stem diameter of about 1–6 mm (Turner 1994). Its leaf blades are narrow and long, about 1.25 cm wide and ranging from 20 to 30 cm in length. The leaves are rough on the upper side, smooth on the lower side, and grow along the stems (Leithead *et al.* 1971) (Figure 3). In maidencane (*Panicum hemitomon*) marshes, the averaged stem density is 255 stems per square meter; in deep water marshes, the stem density is only 18 per square meter; and in mixed shallow marshes (*Eleocharis elongata*, *Sagittaria lancifolia*, *Panicum hemitomon*, and *Pontederia cordata*), the average density is 286 stems per square meter (Turner 1996). The Davis pond marsh is a typical maidencane marsh. Manning's  $n$  in the subtropical marsh is 0.26–0.55 for water hyacinth, and 0.16–0.43 for vegetation of mixed species for flow depth about



**Figure 3** | *Panicum hemitomon* profile ([www.outdooralabama.com/maidencane](http://www.outdooralabama.com/maidencane)).

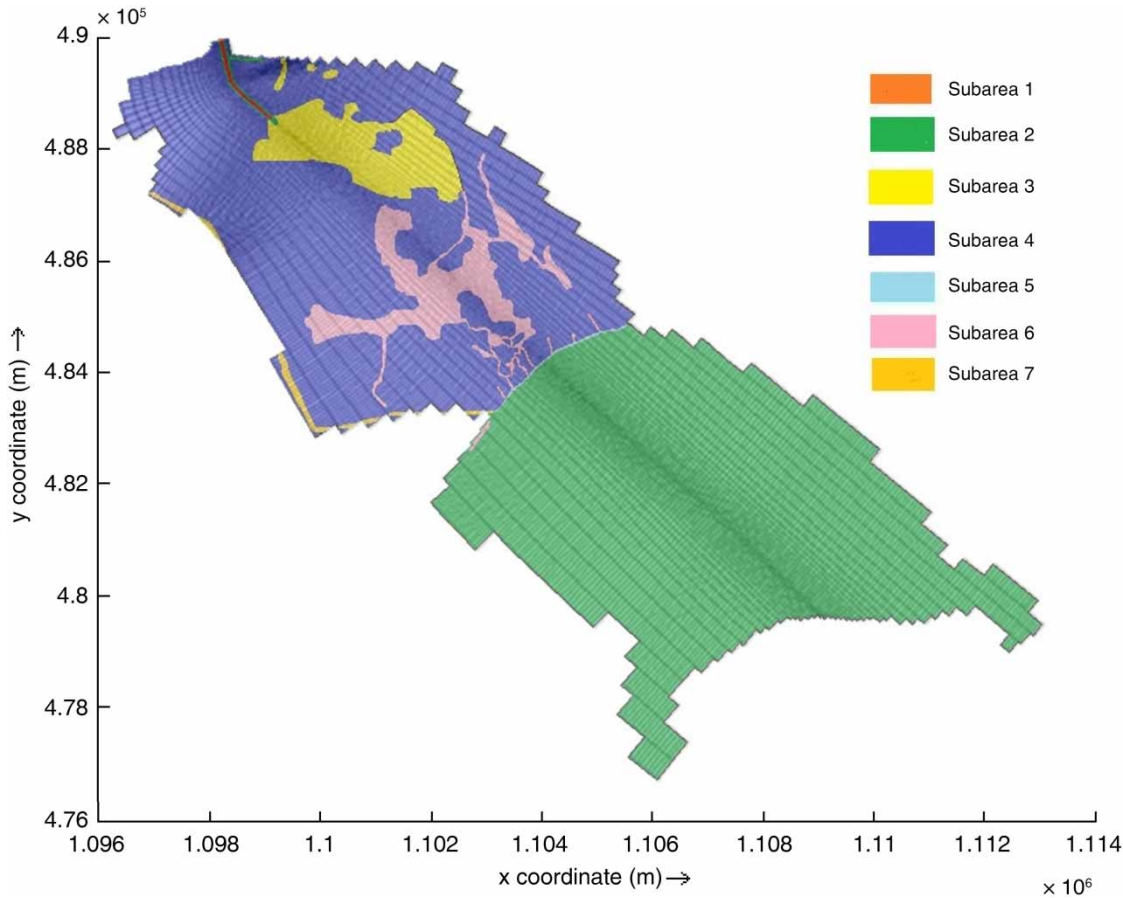


**Figure 4** | Study area subdivision and computation grid.

40–65 cm (Shih & Rahi 1981). The Manning's roughness is inversely calculated by using measured flow depth and velocity in the vegetated area.

## VEGETATION IMPACT

Two common approaches to estimate vegetation roughness were evaluated: a constant  $n$  value, or a time-varying  $n$  or Chezy's  $C$  coefficients for each sub-area. The study area was divided into several sub-areas according to the existence of channels, overbanks, and vegetation height (Figure 4), similar to that in McAlpin *et al.* (2008). The computational grid is overlaid on the subareas in Figure 4. Table 1 summarizes  $n$  values used in the first approach, in which  $n_1$  and  $n_2$  are the maximum values of Manning's roughness coefficient for unvegetated and vegetated sub-areas, respectively (McAlpin *et al.* 2008). Two options were used to vary  $n$

value with time. The equations by Baptist (2005) and Klopstra *et al.* (1997) in Table 2, already incorporated in Delft3D under the Trachytopes function, were used in the first option to calculate the time-dependent  $C$  value. This option treated an individual grass or vegetation as a cylinder with a frontal width equal to its diameter. In this study, the average frontal width was calculated by the number of

**Table 1** | Manning's  $n$ -values for each sub-area used for the first approach

Sub-area	$n_1$	$n_2$
1	0.06	0.10
2	0.06	0.40
3	0.06	0.40
4	0.12	0.82
5	0.12	0.82
6	0.06	0.40
7	0.12	0.82

**Table 2** | List of the empirical equations used to calculate  $n$  and  $C$  values for the second approach

Authors/reference	Equations
Fisher (1992)	$n = n_o + 0.0239 \left( \frac{B^V}{VR} \right)$
Reed <i>et al.</i> (1995)	$n = \beta / \sqrt{H}$
SED2D Model	$n = \frac{n_o}{H^a} (0.3048)^\alpha + n_v \cdot e^{(-H/h_v)}$
Luhar & Nepf (2013)	For $H/h_v \leq 1$ , $n = \left( \frac{C_D a}{2} \right)^{1/2} H^{2/3} g^{-1/2}$ For $H/h_v > 1$ , $n = \left[ \left( \frac{2}{C_*} \right)^{1/2} (1 - B^X)^{3/2} + \left( \frac{2}{C_D a h_v} \right)^{1/2} B^X \right]^{-1} H^{1/6} g^{-1/2}$
Klopstra <i>et al.</i> (1997)	For $H/h_v \leq 1$ , $C = \sqrt{\frac{1}{\frac{C_D a H}{2g} + \frac{1}{C_b^2}}}$ For $H/h_v > 1$ , $C = \frac{1}{H^{3/2}} \left\{ \frac{2}{\sqrt{2A}} \left( \sqrt{C_3 e^{h_v \sqrt{2A}} + u_{v0}^2} - \sqrt{C_3 + u_{v0}^2} \right) \right.$ $+ \frac{u_{v0}}{\sqrt{2A}} \ln \left( \frac{(\sqrt{C_3 e^{h_v \sqrt{2A}} + u_{v0}^2} - u_{v0}) (\sqrt{C_3 + u_{v0}^2} + u_{v0})}{(\sqrt{C_3 e^{h_v \sqrt{2A}} + u_{v0}^2} + u_{v0}) (\sqrt{C_3 + u_{v0}^2} - u_{v0})} \right)$ $\left. + \frac{\sqrt{g(H - (h_v - b))}}{\kappa} \left( (H - (h_v - b)) \ln \left( \frac{H - (h_v - b)}{z_0} \right) - b \ln \left( \frac{b}{z_0} \right) - (H - h_v) \right) \right\}$
Baptist (2005)	For $H/h_v \leq 1$ , $C = C_b$ ; $\lambda = C_D a$ For $H/h_v > 1$ : $C = C_b + \frac{\sqrt{g}}{k} \ln \left( \frac{H}{h_v} \right) \sqrt{1 + \frac{C_D a h_v C_b^2}{2g}}$ ; $\lambda = C_D a \frac{h_v C_b^2}{H C^2}$ <ul style="list-style-type: none"> <li>• For Baptist (2005) equation, a term <math>\left( -\frac{\lambda}{2} u^2 \right)</math> will be added as an additional term in the momentum equations.</li> <li>• For Klopstra <i>et al.</i> (1997) equation;</li> </ul> $A = \frac{a C_D}{2\eta}; C_3 = \frac{2g(H - h_v)}{\eta \sqrt{2A} (e^{h_v \sqrt{2A}} + e^{-h_v \sqrt{2A}})}; b = \frac{1 + \sqrt{1 + \frac{4E_1^2 \kappa^2 (H - h_v)}{g}}}{\frac{2E_1^2 \kappa^2}{g}}; E_1 = \frac{\sqrt{2A} C_3 e^{h_v \sqrt{2A}}}{2\sqrt{C_3 e^{h_v \sqrt{2A}} + u_{v0}^2}};$ $z_0 = b e^{-F}; F = \frac{\kappa \sqrt{C_3 e^{h_v \sqrt{2A}} + u_{v0}^2}}{\sqrt{g(H - (h_v - b))}}; \eta = \max(0.001, 0.0227 h_v^{0.7}); u_{v0} = \sqrt{\frac{h_v}{\frac{C_D h_v a}{2g} + \frac{1}{C_b^2}}}$

leaves, the width of individual leaves, and the stem diameter. In the second option, the rest of the equations in Table 2 were programmed into Delft3D-FLOW program using the Trachytopes function. Because of the lack of detailed vegetation distribution map in the study area, we assumed each sub-area is entirely filled with vegetation of uniform height. With this assumption, the volumetric and cross-sectional blockage factor is equal to the ratio of vegetation height to flow depth.

## DELFT3D-FLOW MODEL FOR THE STUDY AREA

### Computational mesh

The computational grid of the study area was constructed using available geometric and bed elevation data. The bathymetry of the study area was obtained from USACE, and the elevation is referenced to North American Vertical Datum of 1988 (NAVD88). The computational mesh is a structured

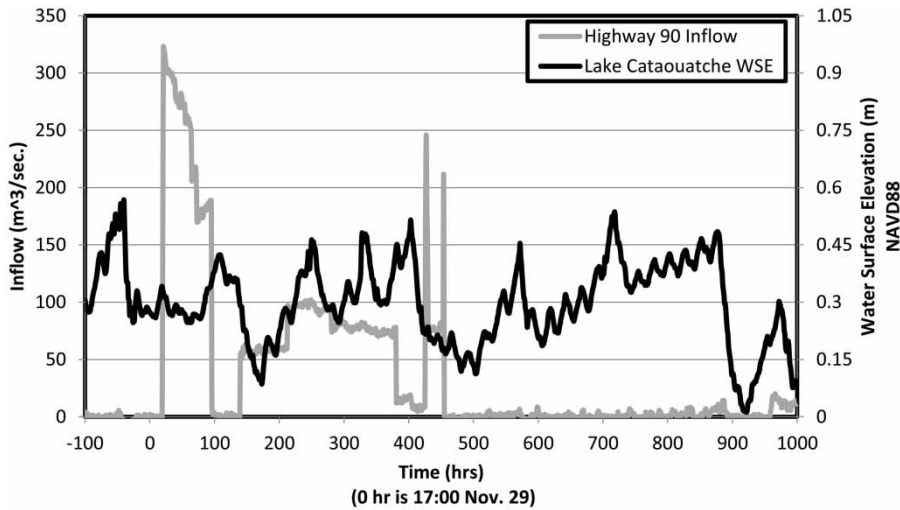


**Figure 5** | Boundary conditions of inflow and tidal stage hydrographs at Highway 90 and Lake Cataouatche gauges respectively.

grid having 299 points in the main flow direction (M), and 53 points in the direction normal to main flow (N), and 15 layers in the vertical (Figure 4). A finer mesh was used in the inlet canal to capture detailed bathymetry because of rapidly varied bed elevation in this region. The maximum grid sizes in main flow and normal to main flow directions are 177.84 and 462.5 m, respectively, and the minimum are 7.13 and 19.19 m, respectively. The grid aspect ratio (N-grid size/M-grid size) ranges from 1.0 to 20.55. The regions of high aspect ratio are located along the border of the study area, where flow is predominately along the N-direction. Because the velocity gradient close to the bed is very high, the distance between  $\sigma$ -layers is smallest at the bottom, and increases toward free surface. The water depth has reached 6.5 m in the inlet canal, and 2.5 m in the other parts during the flood period from 1:00 pm (CDT) on November 30 to 7:00 pm (CDT) on December 3, 2003.

### Boundary conditions

The model was applied to simulate flow from 1:00 p.m. (CDT), November 25, 2003 to 9:00 a.m. (CDT) on January 10, 2004. At the inlet canal, the US Geological Survey (USGS) gauge at Highway 90 recorded flow discharge, which was the upstream boundary condition (Figure 5). Water surface elevations observed at USGS gauge at Lake Cataouatche (Figure 5) were the downstream boundary condition. Slip boundary condition was used on the east, west, and north side levees except

for the inlet. At free surface, shear stress is zero, and at the channel bottom, flow velocity is set as zero.

### Results

Eleven stream gauges are available in the study area (Figure 2). The time step is one minute for both approaches to achieve numerically stable solutions. Table 3 is a summary of vegetation roughness parameters for each subarea using the roughness equations in SED2D model (McAlpin *et al.* 2008). In the equations proposed by Luhar & Nepf (2013), Klopstra *et al.* (1997) and Baptist (2005), the average frontal width of an individual plant is calculated as 2.25 times the leaf width (approximately equal to 1.25 cm) plus the mean stem diameter ( $d = 0.4$  cm). Since the calculated frontal width, symbolized by  $w$ , is 3.2 cm, equal to  $8d$ , this study

**Table 3** | Roughness parameter values for all sub-areas used in SED2D model equation

Sub-area	$n_o$	$h_v$	$n_v$	$\alpha$
1	0.06	0.3048	0.10	0.05
2	0.06	0.381	0.40	0.20
3	0.06	0.3048	0.40	0.20
4	0.12	0.6096	0.82	0.41
5	0.12	0.762	0.82	0.41
6	0.06	0.381	0.40	0.20
7	0.12	0.6856	0.82	0.41

assumes  $8d$  as the vegetation frontal width. Since the  $a$  value is the product of vegetation density and its frontal width, the larger the  $a$  value, the larger the vegetation-induced resistance. In a typical *Panicum hemitomon* grass dominated freshwater marsh in Louisiana, vegetation density is  $255 \text{ stem/m}^2$ , and the average stem diameter is  $0.4 \text{ cm}$ , thus the  $a$ -value is  $8.160 \text{ m}^{-1}$ . This value is within the range,  $1\text{--}10 \text{ m}^{-1}$ , suggested by Luhar *et al.* (2008), Lightbody & Nepf (2006), and Leonard & Luther (1995) for marsh grasses. The drag

coefficient for vegetated channel,  $C_D$ , is equal to 1.0. Shear stress at the interface between vegetated and unvegetated regions is quantified by another drag coefficient, denoted as  $C_s^*$ , and is set as 0.10 (Luhar & Nepf 2013).

In order to quantify the performance of each equation, the simulated WSEs were compared with the observed ones at all gauges in Figures 6 and 7. Root mean square error (RMSE) and Nash–Sutcliffe efficiency (NSE) coefficient between the simulated and observed WSEs were

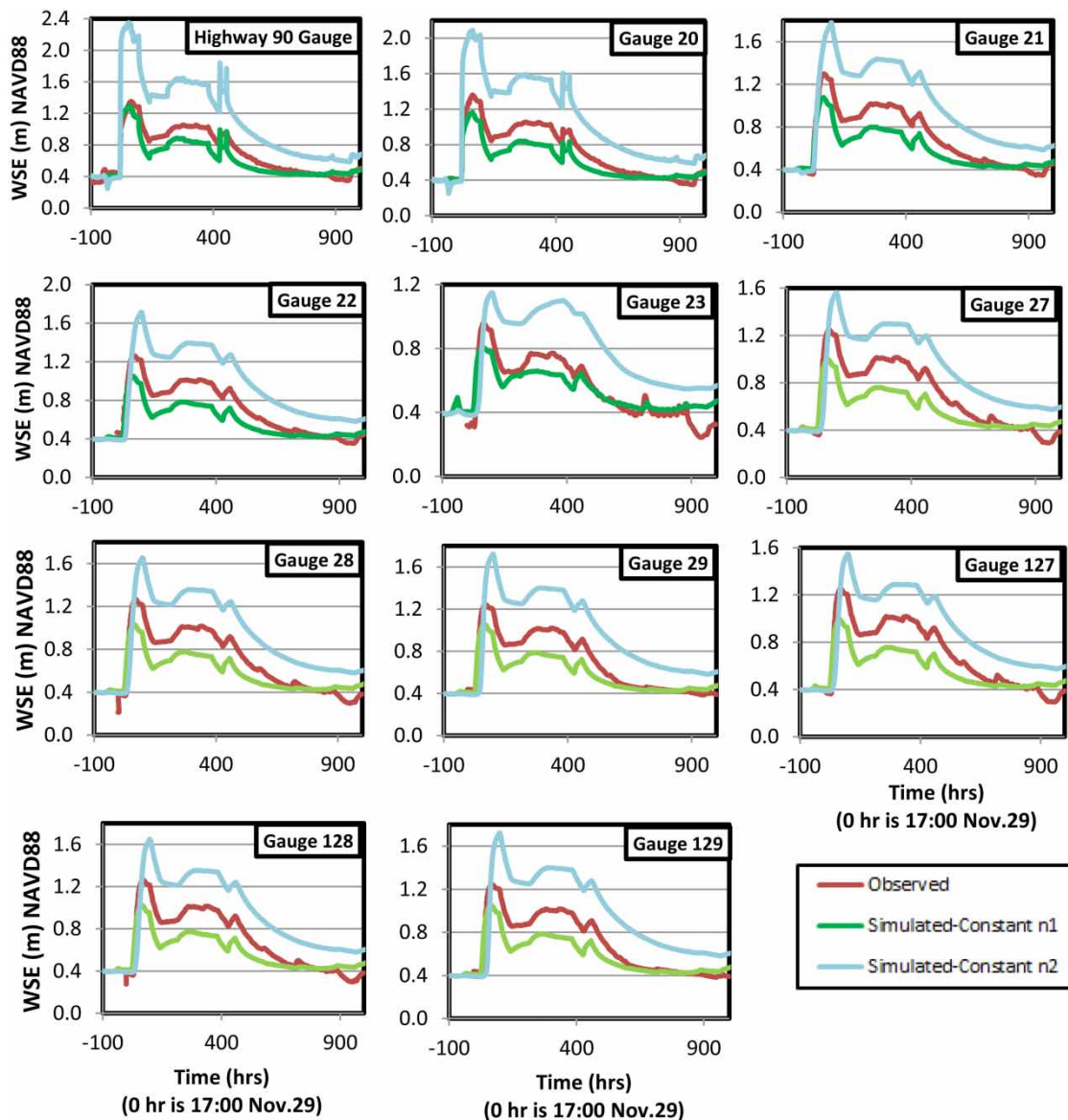


Figure 6 | Observed and simulated WSE for all gauges – first approach.

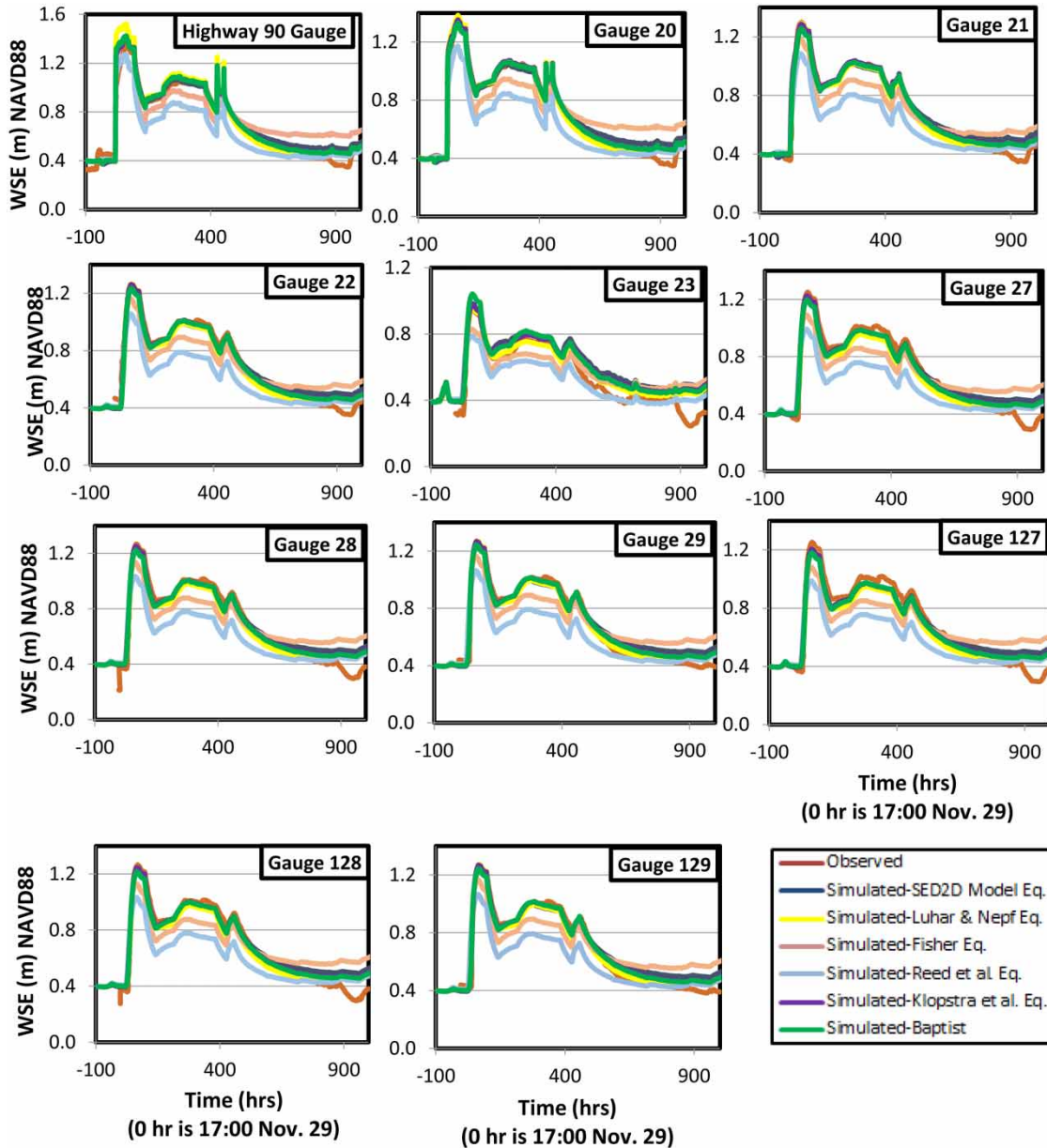


Figure 7 | Observed and simulated WSE for all gauges – second approach

calculated using the following equations:

$$\text{RMSE} = \sqrt{\frac{\sum (S_i - O_i)^2}{N}} \quad (1)$$

$$\text{NSE} = 1 - \frac{\sum (S_i - O_i)^2}{\sum (O_i - \bar{O}_i)^2} \quad (-\infty < \text{NSE} < 1.0) \quad (2)$$

where  $S_i$  and  $O_i$  are  $i$ th simulated and observed value, respectively,  $\bar{O}_i$  is the average of observed values,  $N$  is the total number of observations. The RMSE and NSE values for all the simulations were calculated at all gauges, and their ranges are shown in Figures 8 and 9, respectively. From these figures, one can find the RMSEs using the equation in SED2D model and those using Luhar & Nepf (2013), Klopstra *et al.* (1997), and Baptist (2005) equations

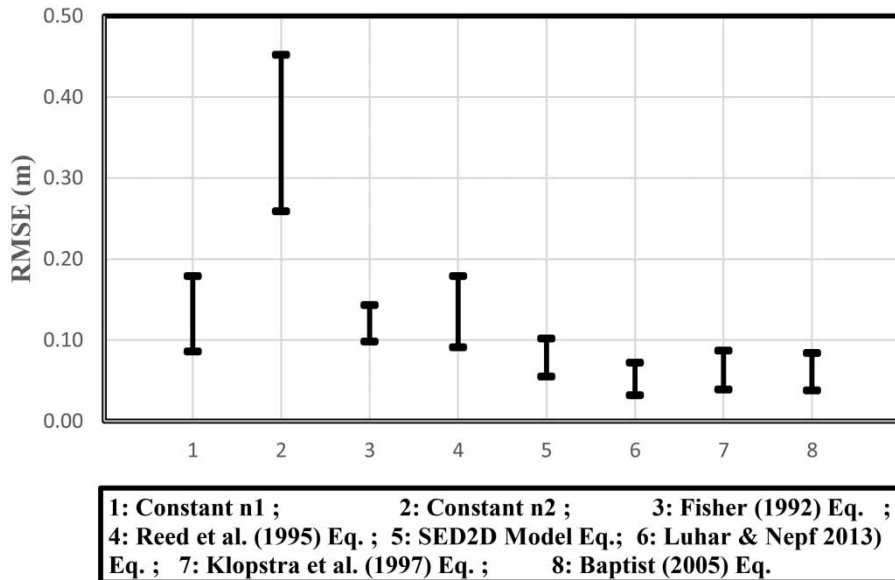


**Figure 8** | Ranges of RMSE for all gauges for both approaches.

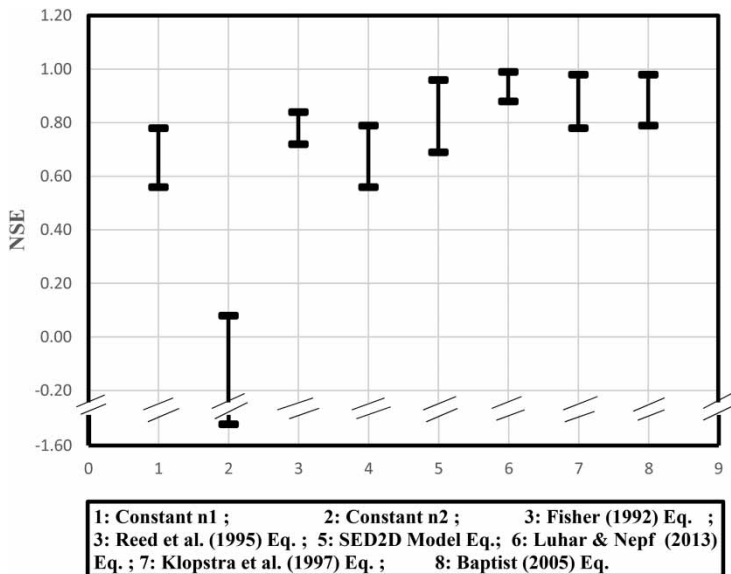


**Figure 9** | Ranges of NSE for all gauges for both approaches.

are relatively small, and their NSEs are closer to 1.0, which indicates that the mean square errors by using these roughness equations are much smaller than the variance of the observations, and the simulated results are more accurate than the results from using other equations.

In the first approach, [Figure 8](#) showed that the range of RMSE for the simulated WSE using the constant Manning roughness for unvegetated channels ( $n_1$ ) is smaller than

the results using Manning's roughness for vegetated channels ( $n_2$ ). The NSE value is also closer to 1.0 for the results using  $n_1$  ([Figure 9](#)). It can be seen from [Figure 7](#) that WSE were underestimated when using the constant  $n_1$ , while they were overestimated when using the constant  $n_2$ . Although the results using  $n_1$  are slightly better than the ones using  $n_2$ , none of them matched the results well at all gauges. Therefore, several  $n$  values between  $n_1$  and

$n_2$  values were selected to re-run the model. However, for each value, the WSEs matched the observation data at one gauge in one time interval but not at other times. Also, WSEs matched the observation data better at some gauges but got worse at the rest. Regardless of the  $n$  value being used, there is no general improvement of modeling results. This excludes the feasibility of using a constant roughness for simulating flow hydrodynamics in a freshwater marsh.

The second approach treated flow roughness as a temporal and spatial variable depending on local flow and vegetation characteristics. The RMSE values using Fisher (1992) and Reed *et al.* (1995) equations are larger (Figure 8) than the results from other equations. The corresponding NSE values using these two equations are also further away from 1.0 than the rest. The equations of Luhar & Nepf (2013), Klopstra *et al.* (1997) and Baptist (2005) yielded the smallest RMSEs, and NSE values are also the closest to 1.0 (Figures 8 and 9). This attributes to the fact that Fisher (1992) and Reed *et al.* (1995) equations do not take the degree of submergence into account, which is essential for differentiating the submerged and emerged vegetation. At low flow depth, the vegetation height is comparable to flow depth, or even emergent. In this condition, vegetation-induced roughness is dominant. However, as flow

depth increases, vegetation becomes submerged and its influence on flow resistance is diminishing (Nepf 2012). When flow depth is orders of magnitude larger than vegetation height, vegetation-induced resistance will converge to a constant (Augustijn *et al.* 2008). Therefore, this study recommends the use of variable Manning roughness to account for vegetation-induced roughness. Figure 10 shows the results from using variable  $n$  values in Luhar & Nepf (2013), Klopstra *et al.* (1997) and Baptist (2005) equations at gauge 21. These three equations have incorporated the vegetation effect by using a vegetation blockage index ( $a$ ). In the next section, the sensitivity of results to modeling parameters, such as  $a$  value, and vertical grid spacing, will be discussed. Nevertheless, the simulation results showed that these three equations are the best choices for simulating vegetation resistance in this estuarine marsh area.

The simulation was run on a PC with Intel (R) Xeon (R) CPU X5550 (two processors) and 32 GB RAM. The CPU times using the first approach were 74,218.84 and 73,815.20 s for the simulation using constant  $n_1$  and  $n_2$ , respectively, whereas they are 72,790.89 and 77,252.20 s using Reed *et al.* (1995) and Klopstra *et al.* (1997) equations, respectively.

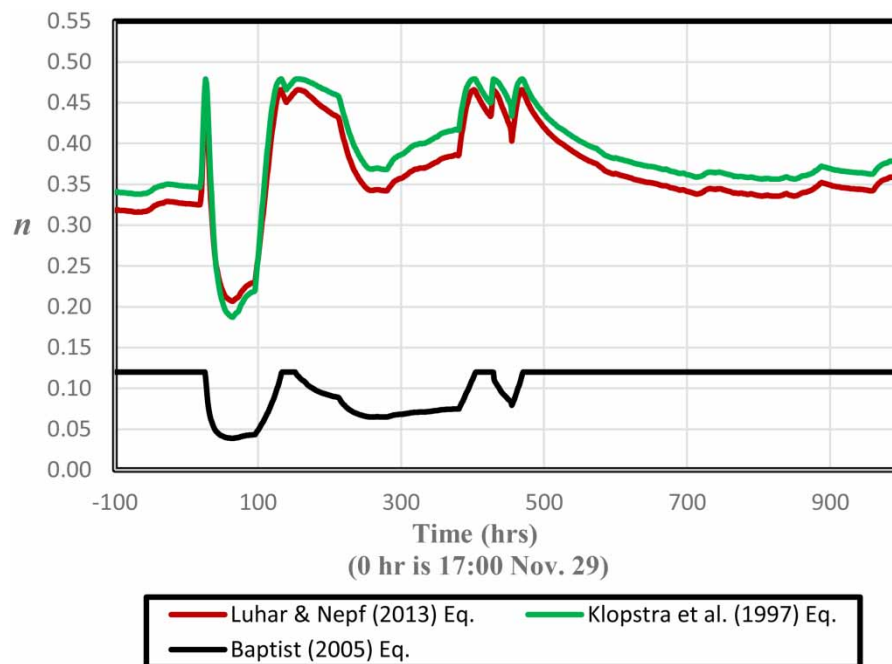


Figure 10 | Changes of  $n$  values for the runs using Luhar & Nepf (2013), Klopstra *et al.* (1997) and Baptist (2005) equations at gauge 21.

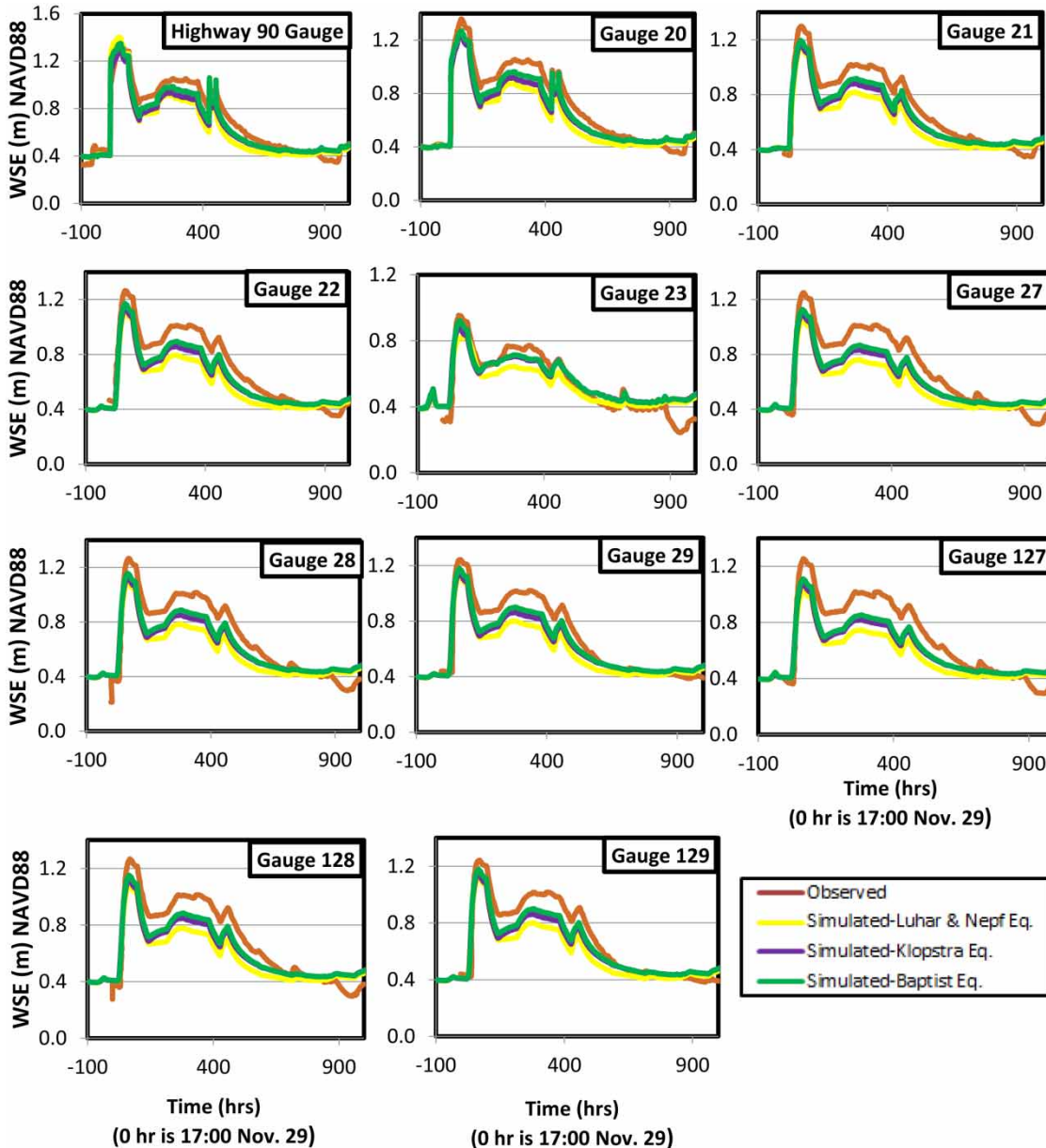


Figure 11 | Observed and simulated WSE for all gauges –  $a = 1.020 \text{ m}^{-1}$ .

## SENSITIVITY ANALYSIS

### Vegetation blockage index ( $a$ value)

Using the equations in Luhar & Nepf (2013), Klopstra *et al.* (1997) and Baptist (2005), results showed the best WSE matches with the observation. However, the results can be sensitive to key parameters (e.g.  $a$  value). To quantify the

sensitivity of modeling results to the variation of  $a$  values, three  $a$  values were selected based on the average frontal width of an individual grass, equal to  $d$ ,  $11d$ , and  $22d$ . Since the average vegetation density is  $255 \text{ stem/m}^2$  and the stem diameter is  $d = 0.4 \text{ cm}$ , the calculated  $a$  values are  $1.020$ ,  $11.220$ , and  $22.440 \text{ m}^{-1}$ , respectively.

The simulated results of WSE using these three  $a$  values were shown with the observed ones at all gauges

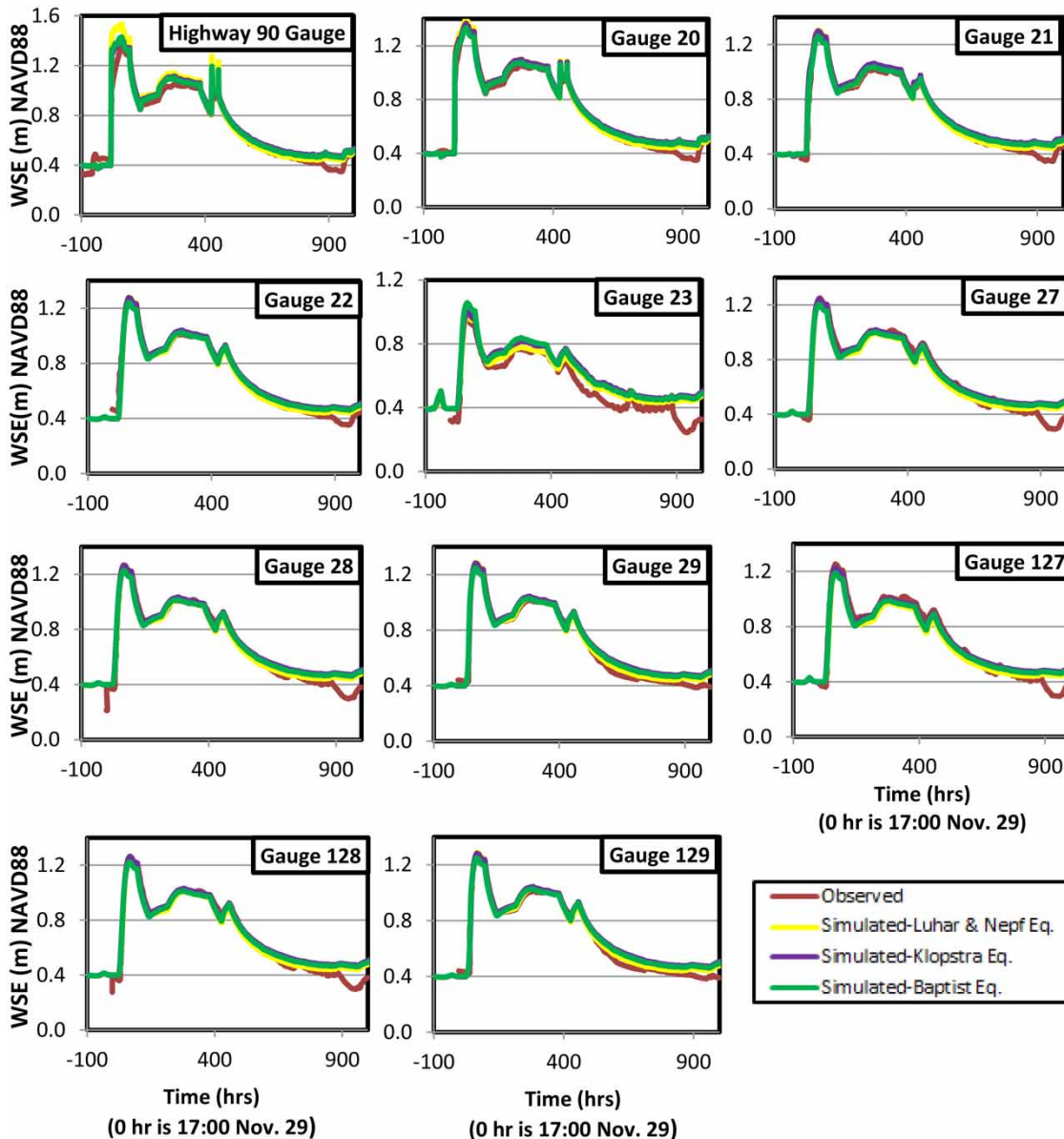


Figure 12 | Observed and simulated WSE for all gauges –  $a = 11.220 \text{ m}^{-1}$ .

in Figures 11–13. When  $a = 1.020 \text{ m}^{-1}$ , the simulated WSEs were underestimated at all gauges (Figure 11), while they were overestimated, especially by the Klopstra *et al.* (1997) equation, when  $a = 22.440 \text{ m}^{-1}$  (Figure 13). The simulated WSEs using  $a = 11.220 \text{ m}^{-1}$  approximately matched the observations (Figure 12). One can find, for  $a = 1.020 \text{ m}^{-1}$ , the averages of RMSE were the largest, and the NSE values were the most distant from 1.0, for all three equations (Figures 14 and 15). For  $a = 11.220 \text{ m}^{-1}$ ,

the averages of RMSE became smaller, and the NSE values were closer to 1.0. For  $a = 11.220$  and  $22.440 \text{ m}^{-1}$ , the averages of RMSE using the Klopstra *et al.* (1997) equation were the largest among three equations, and the NSE values were further distant from 1.0 than the other two equations. This means the Klopstra *et al.* (1997) equation is very sensitive to the variation of  $a$ . Apparently, when  $a$  is equal to  $1.020 \text{ m}^{-1}$ , none of the three equations gave accurate results of WSE. This

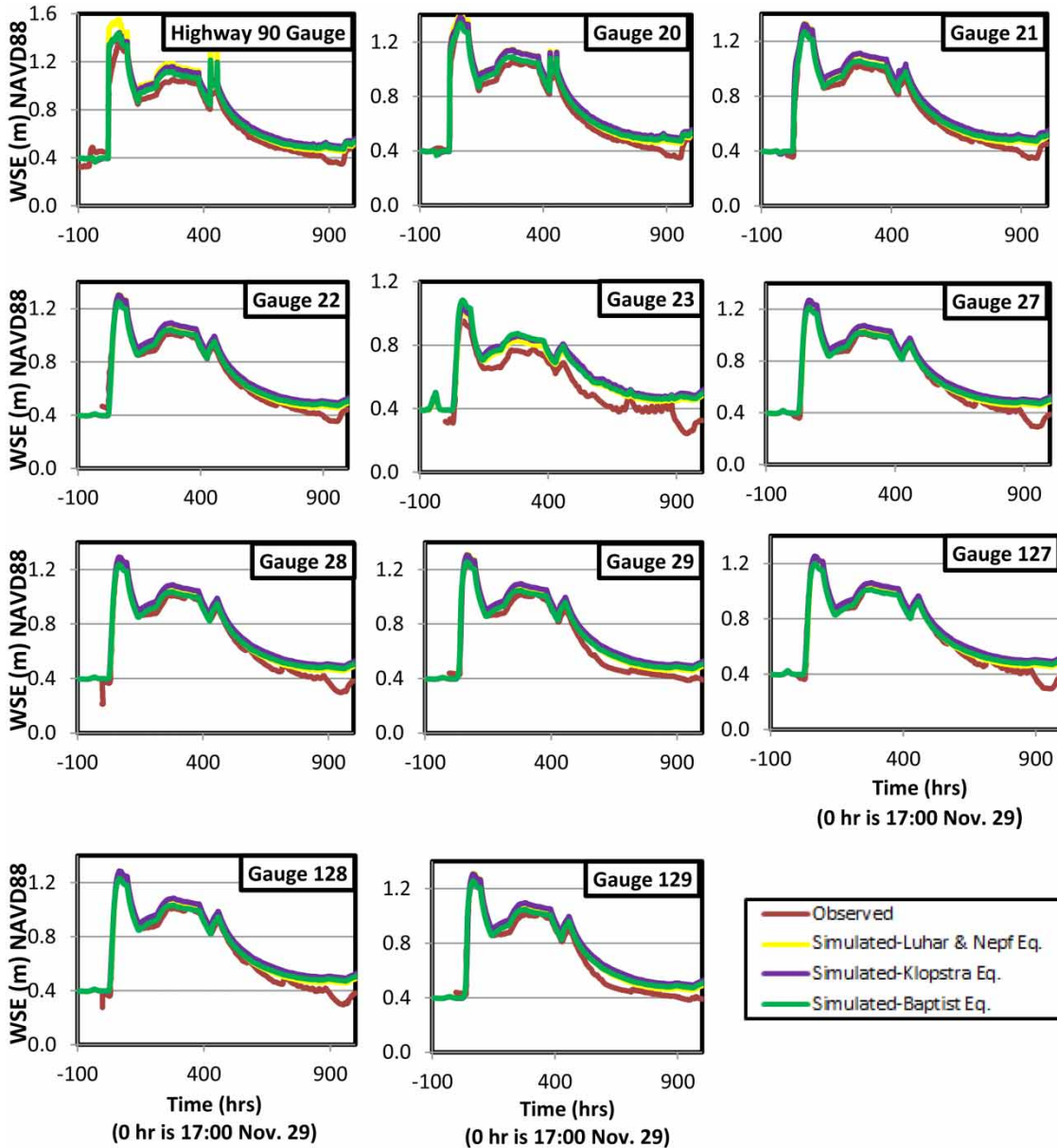


Figure 13 | Observed and simulated WSE for all gauges –  $a = 22.440 \text{ m}^{-1}$ .

implies that the frontal width of an individual grass should be calculated not only by stem diameter but also the number and width of leaves. It can be seen from Figures 8, 9, 14, and 15 that the smallest values of RMSE and the closest NSE values to 1.0 were found when  $a = 8.160$  or  $11.220 \text{ m}^{-1}$ . This confirms that the average frontal width of a grass is between  $8d$  and  $11d$  in a typical maiden-cane marsh with *Panicum hemitomon* as the dominant species.

### Vertical grid selection

As stated earlier, Delft3D-FLOW allows users to choose from two vertical grid systems:  $\sigma$ -grid and Z-grid. The shallow water equations with hydrostatic pressure assumption were solved in both  $\sigma$  and Z-grids. An extension for solving the non-hydrostatic pressure has been added to the Z-grid. All the computational runs conducted until now were using the  $\sigma$ -grid assuming hydrostatic pressure. Since the

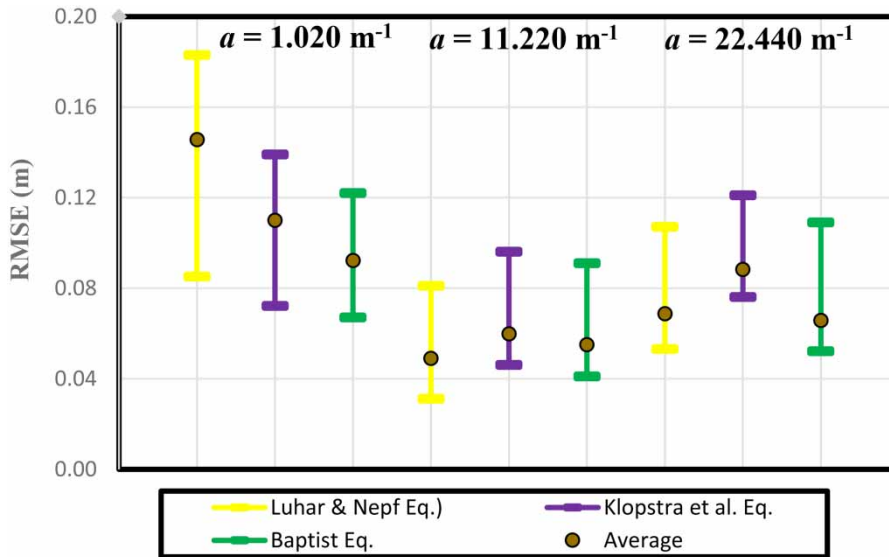


Figure 14 | Ranges and averages of RMSE for all gauges for different  $a$ -values using best three equations.

$\sigma$ -grid forces the convective transport along the channel bottom, it may allow false fluxes between the main channel and floodplain when their elevation difference prohibits such transport. Therefore, the sensitivity of results to the vertical grid selection was performed in this section using Luhar & Nepf (2013) equation. Additional computational runs were conducted using the same computational grid but 15 Z-layers in the vertical plane assuming both

hydrostatic and non-hydrostatic pressure. The time step is 0.1 minute for achieving numerically stable solutions. The CPU times for the runs using the hydrostatic and non-hydrostatic pressure assumptions were 140,968.51 and 211,734.70 s, respectively. The simulated results of WSE at all gauges were compared with the ones using  $\sigma$ -grid and the observations in Figure 16. The results using Z-grid with non-hydrostatic pressure assumption is

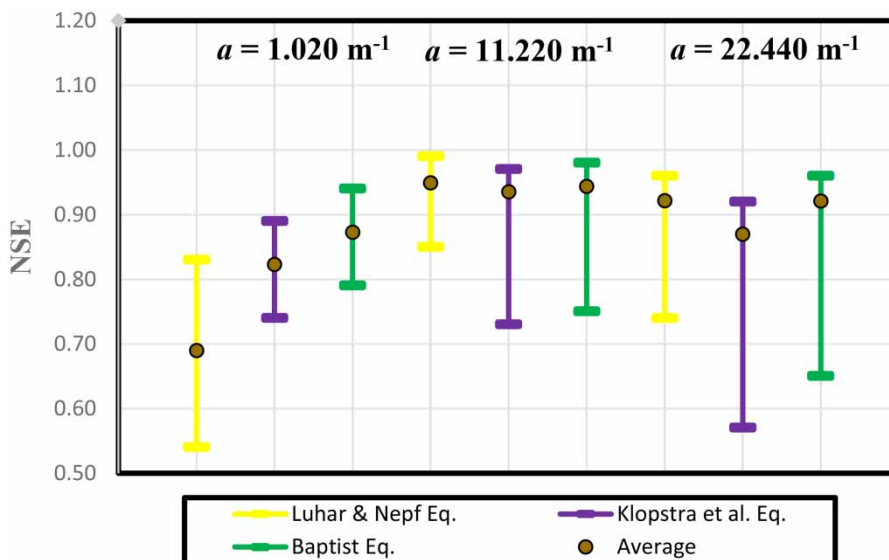
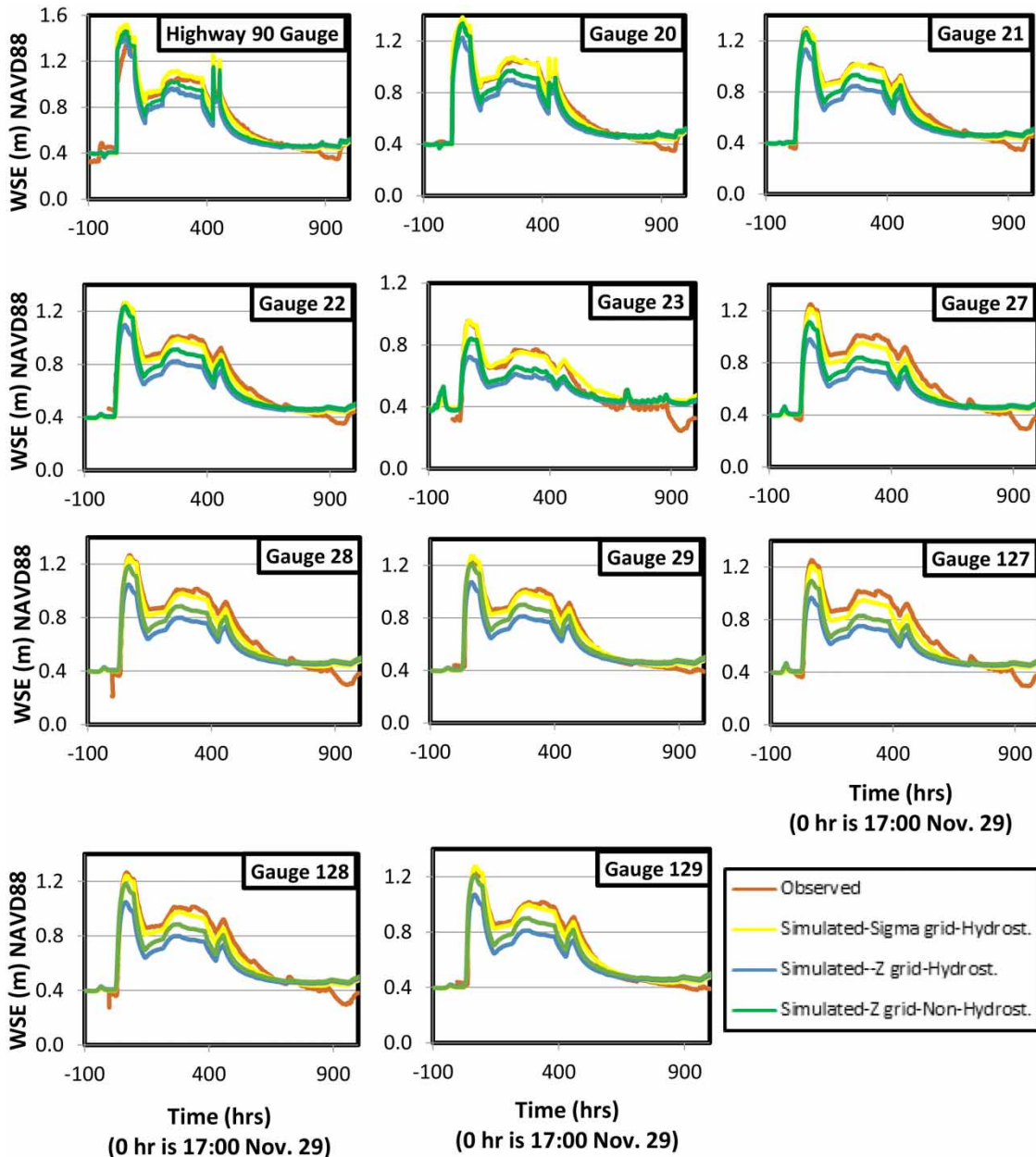


Figure 15 | Ranges and averages of NSE for all gauges for different  $a$ -values using the best three equations.



**Figure 16** | Observed and simulated WSE for all gauges using Luhar & Nepf (2013) equation for different vertical grid selection.

better than those using the hydrostatic pressure assumption. However, these results still deviate far away from the observations, and those using the  $\sigma$ -grid. Figure 17 showed the ranges of RMSE and NSE at all gauges using  $\sigma$ - and Z-grids, which indicated that the RMSE ranges using the  $\sigma$ -grid are the smallest, and the NSE values are closer to 1.0 than both results using the Z-grid. The CPU

time for the simulation using the  $\sigma$ -grid is 76,613.32 s, much less than those using the Z-grid. One major reason is because the  $\sigma$ -grid allows larger time steps (e.g. 1 min) than the Z-grid. Therefore, the Z-grid option did not yield more accurate results but more CPU times than the  $\sigma$ -grid. This study recommends the use of the  $\sigma$ -grid for shallow water marsh application.

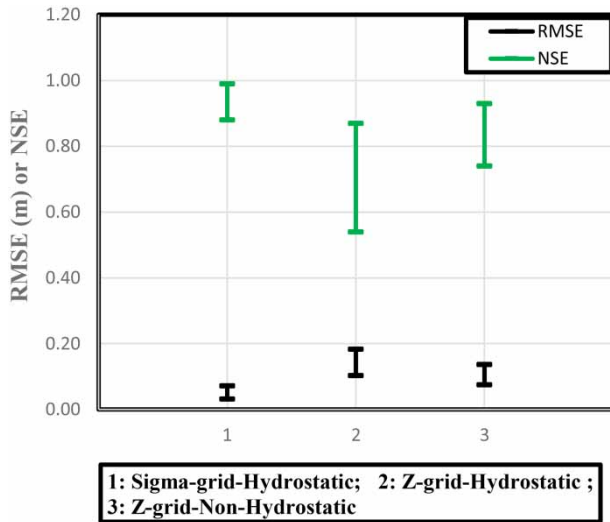


**Figure 17** | Ranges of RMSE and NSE for all gauges using Luhar & Nepf (2013) equation for different vertical grid selection.

## DISCUSSION

Despite significant efforts in quantifying vegetation resistance in estuarine marshes, there is no consensus on which equation is the best. Because of the varieties of vegetation, their complex stem and leaf structures, and their elastic properties in flows, vegetation-induced flow resistance still needs to be determined by using empirical relations in Table 2 or others in the literature. Although this study showed the simulated WSEs best matched the observations using the equations in Luhar & Nepf (2013), Klopstra *et al.* (1997) and Baptist (2005), this conclusion may not be valid for another marsh because vegetation species and ages can alter vegetation's mechanic properties, and thus their influences on flow resistance. Nevertheless, this study found the product of vegetation density and its frontal width is a reliable quantitative measure of vegetation property. Vegetation resistance is dependent on its submergence, and therefore varies with flow depth. Engineers need to validate a selected vegetation resistance equation using observed data of WSE, flow depth, and velocity before adopting it to any field study.

## CONCLUSIONS

This study applied the Delft3D-FLOW model to evaluate the accuracy of various methods for calculating vegetation-

induced resistance in a *maidencane* marsh in the Mississippi River delta. Besides two equations embedded in Delft3D model, four other equations were programmed into the Delft3D-FLOW model. The simulated results of WSE were compared with the corresponding observation at eleven USGS gauges. Results showed that vegetation-induced roughness is a spatial and temporal variable that changes with submergence and vegetation blockage index. If treating flow roughness in each sub-area as constant, the results of WSE deviated considerably from the measurements. On the other hand, when using the equations by Luhar & Nepf (2013), Baptist (2005), and Klopstra *et al.* (1997), reasonable matches with the observed WSE were obtained because these equations have taken the degree of submergence and the vegetation blockage index into account. The best results of WSE were obtained by using a constant vegetation density for the *Panicum hemitomon* vegetation type, and the resulting  $a$  values ranged from 8.160 to 11.220  $\text{m}^{-1}$ . However, this does not warrant the universal applicability of these three equations. Further research is needed to better quantify vegetation property and understand their interactions with flow field.

## ACKNOWLEDGEMENT

This project is partially funded by an Iraq Governmental Graduate Student Training Scholarship. In-kind technical and data support from the Coastal Hydraulics Laboratory in Engineering Research and Development Center, the Corps of Engineers, is greatly appreciated.

## REFERENCES

- Abood, M. M., Yusuf, B., Mohammed, T. A. & Ghazi, A. H. 2006 Manning roughness coefficient for grass-lined channel. *Suranaree J. Sci. Tech.* **13** (4), 317–330.
- Augustijn, D. C. M., Huthoff, F. & van Velzen, E. H. 2008 Comparison of vegetation roughness descriptions. In: *River Flow 2008: Proceedings of the International Conference on Fluvial Hydraulics*. Cesme, Izmir, Turkey, September 3–5.
- Baptist, M. J. 2005 *Modelling Floodplain Biogeomorphology*. Ph.D. Thesis, Delft University of Technology, The Netherlands.
- Chow, V. T. 1959 *Open-Channel Hydraulics*. McGraw-Hill Inc., New York, USA.

- Cowan, W. L. 1956 Estimating hydraulic roughness coefficients. *Agric. Eng.* **37** (7), 473–475.
- Deltares 2011 *Delft3D-FLOW User Manual*, Version 3.15.14499. Rotterdam, The Netherlands. Available from: [http://oss.deltares.nl/documents/183920/185723/Delft3D-FLOW\\_User\\_Manual.pdf](http://oss.deltares.nl/documents/183920/185723/Delft3D-FLOW_User_Manual.pdf).
- Fisher, K. 1992 *The Hydraulic Roughness of Vegetated Channels*. Rep. SR 305. Hydraulics Research Ltd, Wallingford.
- Green, J. C. 2005 Comparison of blockage factors in modeling the resistance of channels containing submerged macrophytes. *River Res. Appl.* **21** (6), 671–686.
- Horstman, E., Dohmen-Janssen, M. & Hulscher, S. 2013 Modeling tidal dynamics in a mangrove creek catchment in Delft3D. *Coast. Dynam.* **2013**, 833–844.
- Klopstra, D., Barneveld, H. J. & Van Noortwijk, J. M. 1996 *Analytisch model hydraulische ruwheid van overstromde moerasvegetatie*. Tech. Rep. PR051, HKV consultants, Lelystad, The Netherlands. Commissioned by Rijkswaterstaat/RIZA, The Netherlands.
- Klopstra, D., Barneveld, D., van Noortwijk, H. J., van Noortwijk, J. M. & van Velzen, E. H. 1997 Analytical model for hydraulic roughness of submerged vegetation. In: *Managing Water: Coping with Scarcity and Abundance: Proceedings of Theme A: the 27th Congress of International Association for Hydraulic Research*, San Francisco, August 10–15, pp. 775–780.
- Leithead, H. L., Yarlett, L. L. & Shifflet, T. N. 1971 *100 Native Forage Grasses in 11 Southern States*. Agric. Handb. US Dep. Agri., Washington, DC, 389 pp.
- Leonard, L. A. & Luther, M. E. 1995 Flow hydrodynamics in tidal marsh canopies. *Limnol. Oceanogr.* **40**, 1474–1484.
- Letter, J. V., Teeter, A. M. & Donnel, B. P. 2011 *User's Guide for SED2D Version 4.5*. US Army Corps of Engineers, Engineering Research and Development Center, Vicksburg, MS. 188 pp.
- Lightbody, A. F. & Nepf, H. M. 2006 Prediction of velocity profiles and longitudinal dispersion in emergent saltmarsh vegetation. *Limnol. Oceanogr.* **51**, 218–228.
- Luhar, M. & Nepf, H. M. 2013 From the blade scale to the reach scale: a characterization of aquatic vegetative drag. *Adv. Water Resour.* **51**, 305–316.
- Luhar, M., Rominger, J. & Nepf, H. M. 2008 Interaction between flow, transport and vegetation spatial structure. *Environ. Fluid Mech.* **8** (5–6), 423–439.
- McAlpin, T. O., Letter Jr, J. V. & Martin, S. K. 2008 *A Hydrodynamic Study of Davis Pond, Near New Orleans, LA*. Rep. / ERDC/CHL TR-08-11, Coast. Hydraul. Lab., US Army Corps of Engineers, Engineering Research and Development Center, Vicksburg, MS, USA.
- Nepf, H. M. 1999 Drag, turbulence, and diffusion in flow through emergent vegetation. *Water Resour. Res.* **35** (2), 479–489.
- Nepf, H. M. 2012 Hydrodynamics of vegetated channels. *J. Hydraul. Res.* **50** (3), 262–279.
- Nepf, H. M., Sullivan, J. A. & Zavistoski, R. A. 1997 A model for diffusion within an emergent vegetation. *Limnol. Oceanogr.* **42** (8), 1735–1745.
- Nikora, V., Lamed, S., Nikora, N., Debnath, K., Cooper, G. & Reid, M. 2008 Hydraulic resistance due to aquatic vegetation in small streams: field study. *J. Hydraul. Eng.* **134** (9), 1326–1332.
- O'Neil, T. 1949 *The Muskrat in the Louisiana Coastal Marshes*. Technical Report. Louisiana Department of Wildlife and Fish, New Orleans, LA, 152 pp.
- Petryk, S. & Bosmajian, G. 1975 Analysis of flow through vegetation. *J. Hydraul. Div.* **101** (7), 871–884.
- Ree, W. D. & Palmer, V. J. 1949 Flow of water in channels protected by vegetative linings. *U.S. Department of Agriculture Technical Bulletin* 967, 115 pp.
- Reed, S. C., Crites, R. W. & Middlebrooks, E. J. 1995 *Natural Systems for Waste Management and Treatment*, 2nd edn. McGraw-Hill Inc., New York, USA.
- Sasser, C. E., Visser, J. M., Mouton, E., Linscombe, J. & Hartley, S. B. 2008 *Vegetation Types in Coastal Louisiana in 2007*. *U.S. Geological Survey Open-File Report 2008*, 1224, 1 sheet, scale 1:550,000.
- Shih, S. F. & Rahi, G. S. 1981 Seasonal variation of Manning's roughness coefficient in a subtropical marsh. *Trans. ASAE* **25** (1), 116–119.
- Stelling, G. S. & van Kester, J. A. T. M. 1994 On the approximation of horizontal gradients in sigma co-ordinates for bathymetry with steep bottom slopes. *Intern. J. Num. Meth. Fluid.* **18**, 915–955.
- Temmerman, S., Bouma, T. J., Govers, G., Wang, Z. B. & De Vries, M. B. 2005 Impact of vegetation on flow routing and sedimentation patterns: three-dimensional modeling for a tidal marsh. *J. Geophys. Res.* **110**, F04019.
- Turner, R. L. 1994 *The Effects of Hydrology on the Population Dynamics of Florida Applesnail (Pomacea paludosa)*. Florida Institute of Technology, Special Publication, SJ94-SP3. Prepared for St. Johns River Water Management District, Melbourne, FL.
- Turner, R. L. 1996 Use of stems of emergent plants for oviposition by the Florida Applesnail, *Pomacea paludosa*, and implications for marsh management. *Flori. Scient.* **59**, 34–49.
- Wu, F.-C., Shen, H. W. & Chou, Y.-J. 1999 Variation of roughness coefficients for unsubmerged and submerged vegetation. *J. Hydraul. Eng.* **125** (9), 934–942.

First received 30 May 2016; accepted in revised form 16 May 2017. Available online 18 July 2017